JOURNAL OF CATALYSIS **159,** 270–279 (1996)
ARTICLE NO. 0088

X-Ray Photoelectron and X-Ray Excited Auger Electron Spectroscopic Analysis of Surface Modifications of Chromia during Heterogeneous Catalyzed Chlorine/Fluorine Exchange

E. Kemnitz,*,[1] A. Kohne,* I. Grohmann,* A. Lippitz,† and W. E. S. Unger†

*Institut für Chemie der Humboldt-Universität zu Berlin, Hessische Str. 1/2, D-10115 Berlin, Germany; and †Bundesanstalt für Materialforschung und-prüfung (BAM), Labor. VIII.23, Unter den Eichen 87, D-12205 Berlin, Germany

Received January 4, 1995; revised October 24, 1995; accepted October 31, 1995

When chromia is employed as a catalyst for heterogeneous chlorine/fluorine exchange reactions drastic modifications in the solid surface regions occur due to chemical reactions with the gas phase. As a result the solid develops its full catalytic activity. Certain amounts of halides (chloride as well as fluoride) are analytically detectable but XRD does not reveal any changes due to small amounts and/or the amorphous character of the surface products. XPS and XAES have been employed to obtain further information on the phases formed during the conditioning process. Different chromium compounds (oxides and fluorides) have been investigated as reference samples. The catalytic behavior has been determined and compared with changes of the photoelectron and Auger electron spectra of the solid samples. From the results it can be stated that a catalytically active phase is formed in all cases during the conditioning process. This phase exhibits chemical and topological properties very similar to β-CrF_3. By contrast, α-CrF_3 is completely inactive catalytically. Explanations are given on the basis of structural differences between the two CrF_3 modifications. © 1996 Academic Press, Inc.

INTRODUCTION

The ozone-depleting chlorine–fluorine carbons (CFCs) are being substituted by their alternatives, the hydrogen–fluorine carbons (HFCs), which have no ozone depletion potential and a substantially shorter atmospheric lifetime. Both classes of compounds can be synthesized by the exchange of fluorine for chlorine in chloroalkanes. For example, CH_2F–CF_3 (HFC-134a), one of the most interesting CFC alternatives, may be prepared from $CHCl{=}{=}CCl_2$ and HF (1–4):

$$C_2HCl_3 \xrightarrow{+HF} C_2H_2Cl_3F \xrightarrow[-HCl]{+HF} C_2H_2Cl_2F_2 \xrightarrow[-HCl]{+HF} C_2H_2ClF_3 \xrightarrow[-HCl]{+HF} C_2H_2F_4. \quad [1]$$

This halogen exchange is thermodynamically favorable but it is hindered from the kinetic point of view. To reach acceptable degrees of conversion it is therefore necessary to employ suitable fluorinating catalysts. Halogenides, oxides and oxyfluorides, respectively, are widely used as heterogeneous fluorinating catalysts. These compounds can be formally considered as Lewis acids. The acid properties are based on the electronic conditions and on coordinatively unsaturated valences of the surface metal atoms.

Most often chromia or alumina are used as fluorinating catalysts (5–10). At the beginning of the conditioning process these oxides undergo considerable changes in the chemical composition and structural constitution of the surface. This effect is independent of the haloalkane used. The changes are caused by the heterogeneous reaction between the surface of the solid and the organic gas phase. As a result the surface achieves full catalytic activity. It is not yet known which processes take place during this period and what phases are formed in the solid surface. The question as to which surface species is responsible for the catalytic behavior is also not answered at this time.

In recent work the influence of the organic educt phase on the kind of surface modification during the conditioning period of several alumina compounds was analyzed more in detail (11, 12). In the present work X-ray photoelectron spectroscopy (XPS) and X-ray excited Auger electron spectroscopy (XAES) have been employed to scrutinize the influence of different haloalkanes on the formation of catalytic active surface species in several chromium compounds employed as catalysts for the halogen exchange reactions.

METHODS

Conditioning of the Catalyst Precursors

The conditioning of the precursors was carried out in a PTFE-lined tubular reactor of nickel (length 400 mm, inner diameter 7 mm) operated under continuous flow conditions

[1] To whom correspondence should be addressed.

0021-9517/96 $18.00

(between 2.5 to 3.5 liter/h). The reactor was heated in a cylindrical resistance oven which was equipped with a temperature control, thus giving temperature fluctuations of $\pm 5°C$. The flow of conditioning haloalkanes was calibrated by flow controllers (MKS Instruments). Before conditioning the samples were dried at 693 K in a predried nitrogen gas stream for 3 h. After drying the reaction temperature was adjusted to 523, 573, or 673 K, respectively, and a constant halocarbon gas flow (residence time: 1 s) passed through the catalyst bed until a constant product distribution in the gas phase was observed. The organic reaction products were determined by gas chromatography using a Chromatron MGC 4000 (fused silica column, 25 m Poraplot Q, detector: FID).

Conditioning Procedure of the Solids Used

α-Cr_2O_3/CFC−12	dried at 693 K for 3 h; conditioned at 573 K with CCl_2F_2
α-Cr_2O_3/HCFC-22	dried at 693 K for 3 h; conditioned at 523 K with $CHClF_2$
α-Cr_2O_3/HCFC-131a	dried at 693 K for 3 h; conditioned at 673 K with $CH_2Cl–CCl_2F$
α-Cr_2O_3/HFC-134	dried at 693 K for 3 h; conditioned at 693 K with $CHF_2–CHF_2$
β-CrF_3/HCFC-131a	dried at 693 K for 3 h; conditioned at 673 K with $CH_2Cl–CCl_2F$
β-(Cr, Al)F_3/HCFC-131a	dried at 693 K for 3 h; conditioned at 673 K with $CH_2Cl–CCl_2F$

XPS Reference Samples and Precursors

α-Cr_2O_3	synthesized via the $(NH_4)_2Cr_2O_7$ volcano reaction structure: corundum specific surface area: 54.6 m^2/g (did not change during drying and conditioning)
β-CrF_3	synthesized by thermal decomposition of $(NH_4)_3CrF_6$ (13) at 763 K structure: hexagonal tungsten bronze (HTB) specific surface area: 7.3 m^2/g
α-CrF_3	commercial product (Riedel de Haen) pa. structure: corundum specific surface area: 5.6 m^2/g
β-(Cr, Al)F_3	synthesized by thermal decomposition of $[Cr(NH_3)_6]AlF_6$ (14) structure: hexagonal tungsten bronze (HTB) specific surface area: 51 m^2/g

Spectroscopy

Photo- and Auger electron spectra were taken by a VG Scientific ESCALAB 200X electron spectrometer. XPS and X-ray excited Auger electron (XAES) narrow scan spectra were acquired at Al$K\alpha$ excitation (15 kV, 20 mA) in FRR mode (CRR 40). The spectrometer energy scale was calibrated employing the procedure and binding energy (BE) reference data recommended by Anthony and Seah (15).

The sample powders were prepared on standard VG sample stubs with the help of double-sided adhesive films. Before recording spectra, the samples were stored to degas for 1 night at 10^{-7} mbar within the extended prep-lock of the ESCALAB. The vacuum within the spectrometer chamber during measurements was better than 10^{-8} mbar. Binding or kinetic energy data were referred to the aliphatic carbon species C 1*s* BE at 284.8 eV (16). XP spectral analysis was performed by peak fitting employing the respective procedures of the SCIENTA ESCA-300 data system.

Special attention was focused on fitting the Cr(III) 2*p* spectra. Their primary structure is characterized by a doublet due to spin-orbit coupling. These two main peaks have strong secondary satellite structures on the high binding energy side. The Cr $2p_{3/2}$ satellite peak is superimposed by the Cr $2p_{1/2}$ photoelectron peak, thus giving a virtual three-peak spectrum (cf. Fig. 1). The problem of analyzing these spectra was solved by setting up fits with equal satellite distances to the respective Cr 2*p* peaks and by using the theoretical spin-orbit area ratio. X-ray contributions arising from the $K\alpha_{3,4}$ lines were also taken into account as well as the existence of OH groups on the surface of all Cr_2O_3 samples. The detailed strategy developed for fitting Cr 2*p* and Cr($L_3M_{23}V$) spectra is given in Ref. (17). The resulting spin-orbit splittings, satellite shifts, and satellite intensities with respect to the main peaks (I_s/I_m) are given in Tables 1 and 2.

For an estimation of the relative intensities (atomic percentage ratios) we used Scofield's cross sections (18), inelastic electron mean free path lengths $\sim E_{kin}^{0.7}$ and a transmission $\sim E_{kin}$. The error of these data is estimated to be better than $\pm 10\%$.

RESULTS

The Conditioning Process of Chromia Precursors

Chromia is often used as the heterogeneous catalyst for different kinds of catalyzed chlorine/fluorine exchange reactions. Among them are (i) fluorination reactions of halocarbons with gaseous hydrogen fluoride, (ii) dismutation reactions, especially of C_1-CFCs and HCFCs, and (iii) isomerization reactions, especially of C_2-halocarbons. These reactions occur in both systems, the former CFCs as well as their alternatives, the HFCs.

Previous investigations of the dismutation reaction of CCl_2F_2 (19, 27) revealed the requirement of a "formation" or "conditioning" process for α-Cr_2O_3 by a haloalkane exposure to reach final catalytic activity. Consequently, a characteristic time-dependent change of the gaseous reaction product concentrations can be observed by GC. In addition to the dismutation products CCl_4, CCl_3F, and $CClF_3$, there is formation of CO_2, HF, and HCl. The latter are degradation products of the haloalkane reactions with Cr_2O_3. A decrease in the degradation products vs time was observed. After about 20 min CO_2, HF, and HCl completely disappear and the highest catalytic activity of the solid is reached. Subsequently, only the dismutation products can

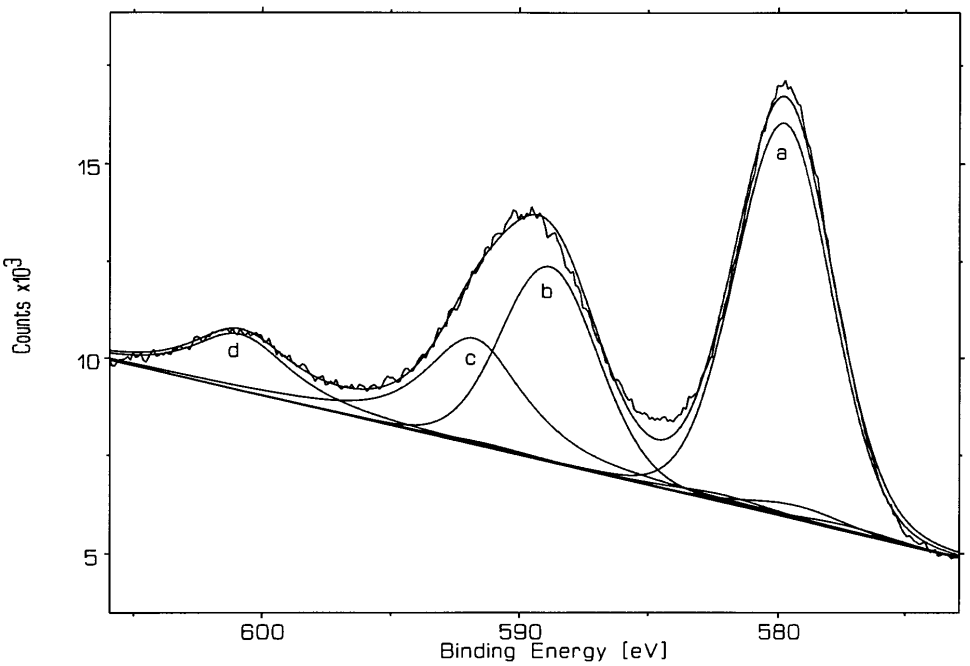

FIG. 1. Cr $2p$ spectrum of β-CrF_3: (a) Cr $2p_{3/2}$ photoelectron peak; (b) Cr $2p_{1/2}$ photoelectron peak; (c) satellite of Cr $2p_{3/2}$; (d) satellite of Cr $2p_{1/2}$.

be observed. This activation behavior can be shown by the changes of the organic haloalkane product distribution with the activation time as given in Fig. 2. The degradative reactions are accompanied by a partial halogenation of the chromia surface. Chemical analysis revealed 0.5 wt% fluoride and 0.4 wt% chloride in the conditioned chromia. X-ray diffraction analysis did not reveal any changes for these chromia samples. Thus the changes should be strongly concentrated at the surface or the new phases are X-ray amorphous.

We also employed chromia as a catalyst for the dismutation reaction of $CHClF_2$ under similar conditions (28). As verified by Fig. 3, this reaction system seems to be somewhat similar to the former one, but the conditioning period takes less time. Due to the hydrogen atom in the $CHClF_2$ molecule this haloalkane is less stable than a CCl_2F_2 molecule and this, therefore, results in a shortening of the conditioning period. It can be seen from the product concentration curves characterizing the conditioning period that (i) a heterogeneous reaction between the solid and

TABLE 1

XP Spectroscopic Data of Reference Samples (Static Charge Reference: Aliphatic C 1*s* with BE = 284.8 eV; Δ(BE) and Δ(KE) Estimated to be ± 0.2 eV)

Samples	BE[a] Cr $2p_{3/2}$/ FWHM[b] (eV)	Δ(BE) Cr $2p$ (1/2-3/2)[c] (eV)	Satellite shifts (eV)	I_sI_m[d]	KE[e] Cr $L_3M_{23}V$ (eV)	$\alpha\prime_{Cr}$[f] (eV)	BE[a] F 1*s*/ FWHM (eV)	KE[e] F $KL_{23}L_{23}$ (eV)	α'_F[f] (eV)
α-Cr_2O_3	576.1/3.5	9.4	11.0	0.21	528.9	1105.0			
α-CrF_3	580.1/3.6	9.3	11.9	0.29	525.4	1105.5	685.4/2.4	655.6	1341.0
β-CrF_3	579.8/4.4	9.1	12.0	0.34	525.7	1105.5	685.6/2.6	655.5	1341.1
β-(Cr, Al)F_3	580.7/4.3 (73%)	9.1	12.0	0.34	525.0	1105.7	686.4/2.9	654.0	1340.4
	576.8/3.6 (27%)	9.4	11.1	0.19					
β-AlF_3							687.8/3.0	651.7	1339.5

[a] BE, binding energy.
[b] FWHM, full width at half-maximum.
[c] Δ(BE) Cr $2p$ (1/2-3/2), spin-orbit splitting of the Cr $2p$ peak.
[d] I_s/I_m, satellite intensities with respect to the main peaks.
[e] KE, kinetic energy.
[f] α', modified Auger parameter.

TABLE 2

XP Spectroscopic Data of Samples Modified with Halocarbons (Static Charge Reference: Aliphatic C 1*s* with BE = 284.8 eV; Δ(BE) and Δ(KE) Estimated to be ± 0.2 eV)

Samples	BE Cr $2p_{3/2}$/ FWHM (eV)	Δ(BE) Cr 2*p* (1/2-3/2) (eV)	Satellite shifts (eV)	I_s/I_m	KE Cr $L_3M_{23}V$ (eV)	α'_{Cr} (eV)	BE F 1*s*/ FWHM (eV)	KE F $KL_{23}L_{23}$ (eV)	α'_F (eV)
α-Cr_2O_3/12[a]	576.8/3.8	9.4	11.1	0.21	528.1	1104.9	685.1/2.4	657.0	1342.1
α-Cr_2O_3/22[b]	576.8/3.5	9.5	11.1	0.21	528.0	1104.8	685.0/2.3	657.0	1342.0
α-Cr_2O_3/131a[c]	576.8/3.8	9.4	11.3	0.21	527.9	1104.7	684.9/2.4	657.0	1341.9
α-Cr_2O_3/134[d]	576.9/3.7	9.4	11.3	0.17	528.1	1105.0	684.9/2.5	657.0	1341.9
β-CrF_3/131a	580.4/4.0	9.2	11.9	0.30	525.2	1105.6	685.8/2.7	655.0	1340.8
β-(Cr, Al)F_3/131a	580.5/4.3 (85%)	9.1	12.0	0.34	525.1	1105.6	686.3/2.9	654.2	1340.5
	576.8/3.6 (15%)	9.4	11.1	0.19					

[a] Modified with CCl_2F_2 at 573 K.
[b] Modified with $CHClF_2$ at 523 K.
[c] Modified with CH_2Cl–CCl_2F at 673 K.
[d] Modified with CHF_2–CHF_2 at 673 K.

the gas phase occurs, and (ii) dismutation reactions can be observed (small at the beginning but rapidly increasing with time of exposure). During this period a higher content of fluorinated organic products appears in correlation with the chlorinated dismutation products. It was proved that this is accompanied by a marked release of HCl, thus explaining the distorted chlorine/fluorine balance in the gas phase. In addition HF is formed but, due to its much higher reactivity, it reacts immediately with chromia forming chromium fluoride. After about 6 min the conditioning process is nearly finished and consequently the dismutation reaction occurs exclusively (the chlorine/fluorine balance in the organic gas phase equals the theoretically expected value). As already shown for CCl_2F_2, the conditioning period for $CHClF_2$ exposure results in its dismutation products and the degradation products CO, HCl, and HF. The latter are formed with enhanced probability. Consequently, the presence of higher amounts of HF and HCl causes a faster halogenation of the chromia surface.

Considering HFC-134a ($CH_2F{=}{=}CF_3$), which is actually an interesting CFC alternative, this molecule is again less stable than $CHClF_2$ in the presence of an active fluorinating catalyst. We also investigated the isomerization reactions of the symmetric HFC-134 to the asymmetric isomer HFC-134a in the presence of a chromia catalyst (29). This isomerization reaction proceeds via the elimination of HF

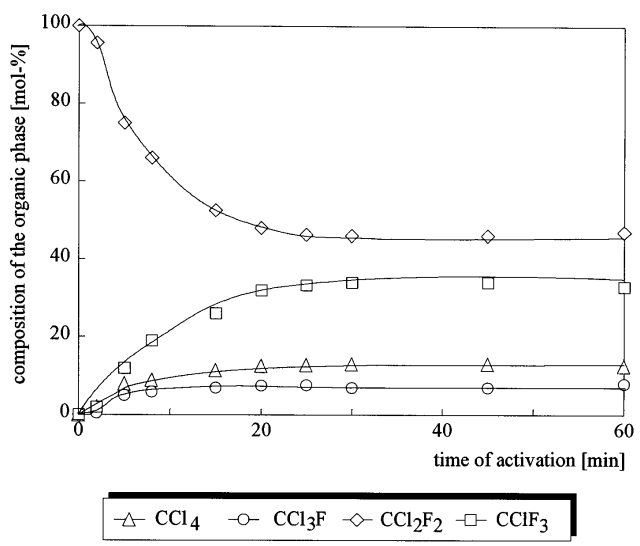

FIG. 2. Conditioning of α-Cr_2O_3 using CCl_2F_2: change of the concentrations of the dismutation products depending on the reaction time at 573 K.

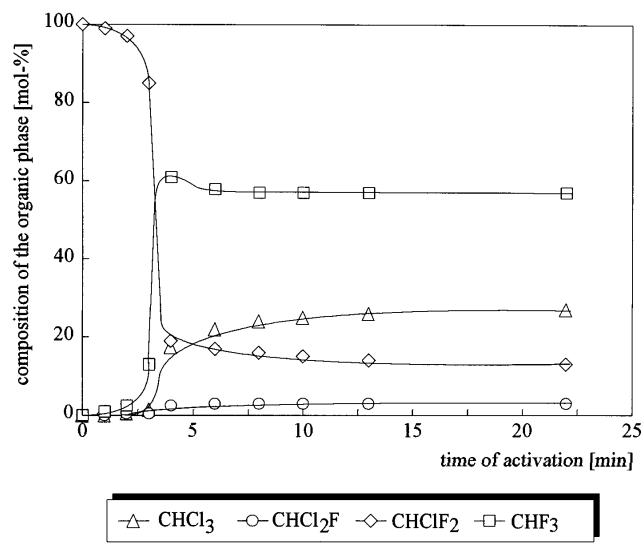

FIG. 3. Conditioning of α-Cr_2O_3 using $CHClF_2$: change of the concentrations of the dismutation products depending on the reaction time at 523 K.

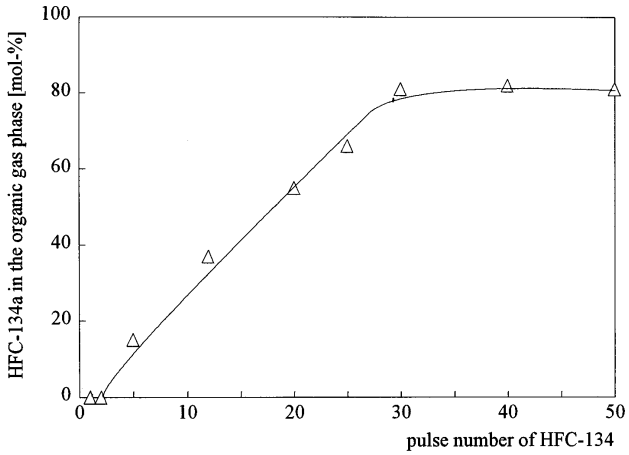

FIG. 4. Conditioning of α-Cr_2O_3 using HFC-134: concentration of the isomerization product HFC-134a depending on the pulse number at 693 K (pulse volume 0.5 ml/stp.).

from CHF_2–CHF_2 forming trifluoroethylene which again recombines with HF according to the Markovnikov rule forming CH_2F–CF_3.

$$CHF_2\text{–}CHF_2 \rightarrow CHF{=}CF_2 + HF \rightarrow CH_2F\text{–}CF_3 \qquad [2]$$

Also in this reaction system a reaction between chromia and HFC-134 forming fluorinated species at the surface of the solid takes place. In the first reaction period a higher catalytic activity of chromia is observed. The enormous amounts of available HF for this system cause a short conditioning period, as shown in Fig. 4. In order to follow these very fast activity changes of chromia we used a pulse technique. The difference from a continuous haloalkane gas flow, used for both other haloalkanes (CCl_2F_2 and $CHClF_2$), is that we used an inert carrier gas flow (N_2) into which pulses of the HFC-134 were added. In this way we were able to follow accurately the conditioning process for this system. Figure 4 verifies that during the first two pulses no isomerization products (HFC-134a) could be observed. After only slight fluorination of the surface a certain catalytic activity appears which continuously increases with further fluorination. After about 30 pulses of the conditioning gas (HFC-134) the partially fluorinated catalyst achieves its full catalyst activity.

If one employs alumina as a catalyst instead of chromia the same conditioning has to be carried out until the final catalytic activity is achieved. For example, in the first step of the dismutation reactions of $CHClF_2$ on γ-Al_2O_3 the solid phase is fluorinated, due to similar heterogeneous solid–gas reactions. In contrast to the chromia system finally one obtains a much higher content of halogenated species at the surface. This strong difference can be easily explained by the enormous difference in the thermodynamic driving force for the reaction of haloalkanes with alumina or chromia. In contrast to alumina, where the formation of Al–F bonds is strongly favored over that of Al–Cl bonds from the reaction of CCl_2F_2 with chromia the enthalpy of reaction $\Delta_R H$ is on the same order of magnitude for the formation of both Cr–F and Cr–Cl bonds.

$$Al_2O_3{+}3CCl_2F_2 \rightarrow 2AlF_3{+}3COCl_2 \quad \Delta_R H = -560 \text{ kJ/mol} \qquad [3]$$

$$Al_2O_3{+}3CCl_2F_2 \rightarrow 2AlCl_3{+}3COF_2 \quad \Delta_R H = -253 \text{ kJ/mol} \qquad [4]$$

$$Cr_2O_3{+}3CCl_2F_2 \rightarrow 2CrF_3{+}3COCl_2 \quad \Delta_R H = -417 \text{ kJ/mol} \qquad [5]$$

$$Cr_2O_3{+}3CCl_2F_2 \rightarrow 2CrCl_3{+}3COF_2 \quad \Delta_R H = -468 \text{ kJ/mol} \qquad [6]$$

Quite different catalytic behavior can be observed in the case of chromium fluoride. α-CrF_3 is nearly catalytically inactive. Even after a preconditioning with CCl_2F_2 of 3 h the catalytic activity was not increased. On the contrary, β-CrF_3, which is described as HTB-CrF_3 due to its structural similarity to hexagonal tungsten bronzes (20), is immediately catalytically active without any formation process. There are no indications for any reactions with CCl_2F_2, which seems reasonable from the chemical point of view. β-(Cr, Al)F_3 shows analogous behavior.

In the chromia system X-ray investigations reveal no evidence for any modifications in the bulk. To obtain distinctive information regarding the surface phases formed during the formation process, XPS and XAES have been employed.

The same method was used to monitor the effect of different gas phases (CFCs, HFCs, C_1- or C_2-haloalkanes) applied for the activation of Cr_2O_3.

XPS and XAES of Reference Samples

Analysis of the binding energy changes in XP spectra for chromia surfaces following exposure to haloalkanes requires the use of reference materials as standards. In Table 1 XPS and XAES data of α-Cr_2O_3, α-CrF_3, β-CrF_3 and β-AlF_3 are summarized.

For comparison, a β-(Cr, Al)F_3 sample is included in Table 1. This sample was not a single-phase one. Its surface contains about 27% of a chromium–oxygen compound, probably a chromium hydroxyfluoride. In order to estimate a correct Cr $2p_{3/2}$ binding energy value a superposition of two chromium spectra characteristic of chromium in Cr_2O_3 and β-CrF_3 was used for fitting these spectra. This fitting procedure was rather complex this giving an increased scatter of optimized binding energy data.

To obtain a more sophisticated fingerprinting the spectroscopic data are presented as so-called "chemical state plots" following Wagner and Joshi (21). In these plots binding energies (BE) of the photoelectrons for an element are

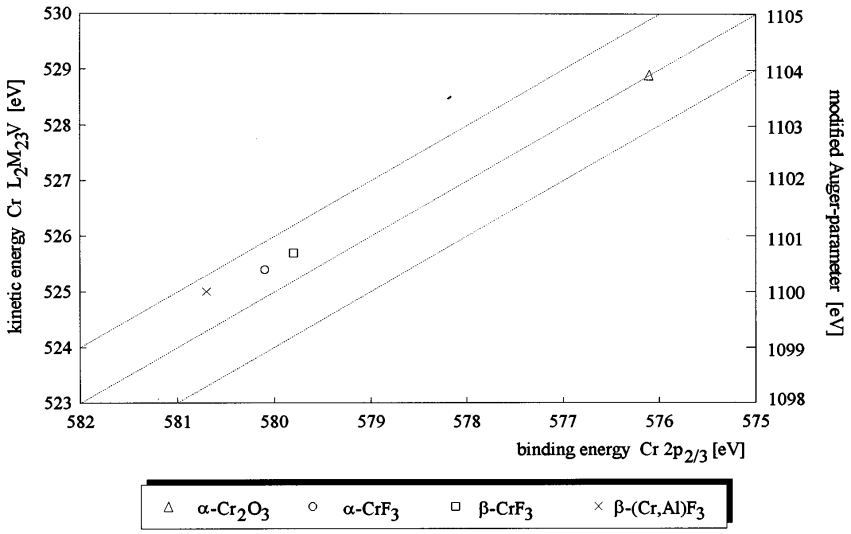

FIG. 5. Chromium chemical state plot for reference samples (Static charge reference C 1*s*: 284.8 eV).

plotted against the kinetic energy (KE) of the respective Auger electrons. The modified Auger parameter data, carrying additional analytical information, are also included. More details on the concept of the chemical state plot are given in a previous paper (11).

In the chemical state plot in Fig. 5 Cr data measured with the reference samples are summarized. The existence of two principal regions of the data can be derived. One region is characteristic for chromium oxide bonds whereas the other, characterized by binding energies around 580 eV, is occupied by chromium fluorine bond species. These results are consistent with the scattered data which one can find in the literature (cf. Table 3).

A chemical state plot for fluorine in the reference samples is given in Fig. 6 which includes also AlF_3 data (cf. Ref. (11)). The different bond strengths of Cr–F and Al–F bonds are the reason for the well separated places of α-CrF_3 and the β-CrF_3 on the one hand and β-AlF_3 on the other. The position of the β-(Cr, Al)F_3 sample data in the plot is of particular interest. As expected, we find its F data between those characteristic of β-CrF_3 and β-AlF_3.

XPS and XAES Results Obtained for Haloalkane Exposed Samples

α-Cr_2O_3. α-Cr_2O_3 has been activated with CCl_2F_2 (CFC-12), $CHClF_2$ (HCFC-22), CH_2Cl–CCl_2F (HCFC-

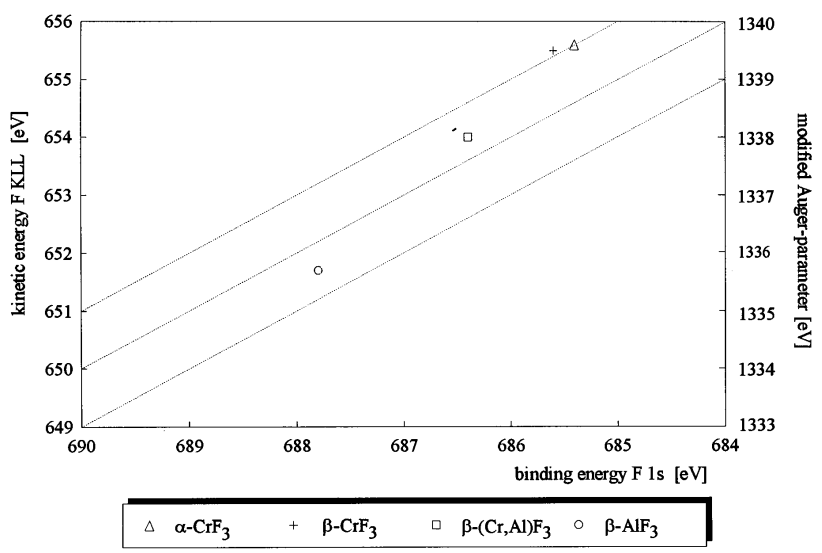

FIG. 6. Fluorine chemical state plot for reference samples (Static charge reference C 1*s*: 284.8 eV).

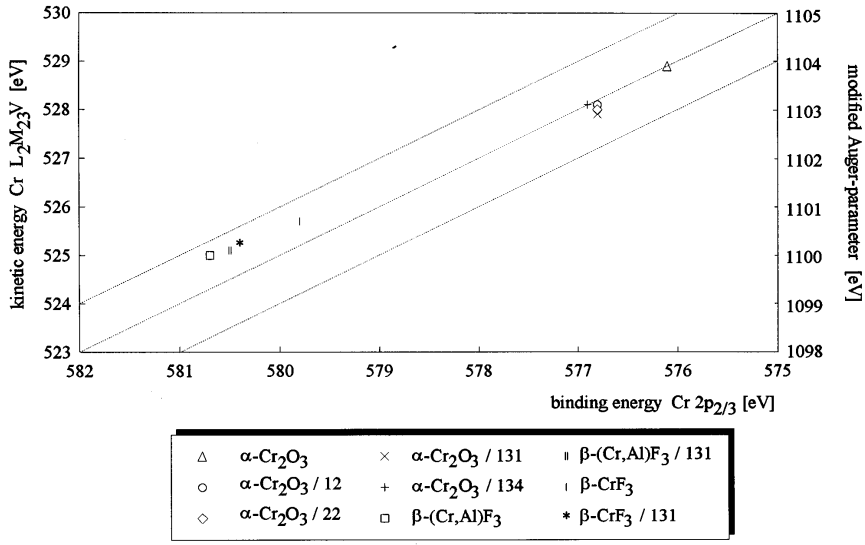

FIG. 7. Chromium chemical state plot for Cr oxide and fluoride samples before and after activation with halocarbons (Static charge reference C 1*s*: 284.8 eV).

131a), or CHF_2–CHF_2 (HFC-134). All chromia samples, activated with these haloalkanes according to the procedure described above, were found to be catalytically active. X-ray analysis *did not reveal any differences* between the precursor chromia and samples which were exposed to haloalkanes.

There are also no differences between these activated chromia samples when the Cr or the F chemical state plots are considered (cf. Figs. 7 and 8). The spin-orbit splitting, satellite shifts, and intensities are very similar to the data of untreated α-Cr_2O_3 (cf. Table 2). In all cases the activation procedure results in a shift of the Cr $2p_{3/2}$ BE data from 576.1 eV, the pure Cr_2O_3 value, to 576.8 eV. This shift can be explained by a partial halogenation of surface chromium atoms. The respective F/Cr surface concentration ratios are given in Table 4.

Additionally, besides fluorine-containing species, we found chlorinated species when chlorine-containing halocarbons were used for the activation procedure (Table 4).

Fluorides with HTB-Structure

It is well known from activity investigations (27) that the structurally isotypic β-CrF_3 and β-(Cr, Al)F_3 compounds are immediately catalytically active. These systems exhibit

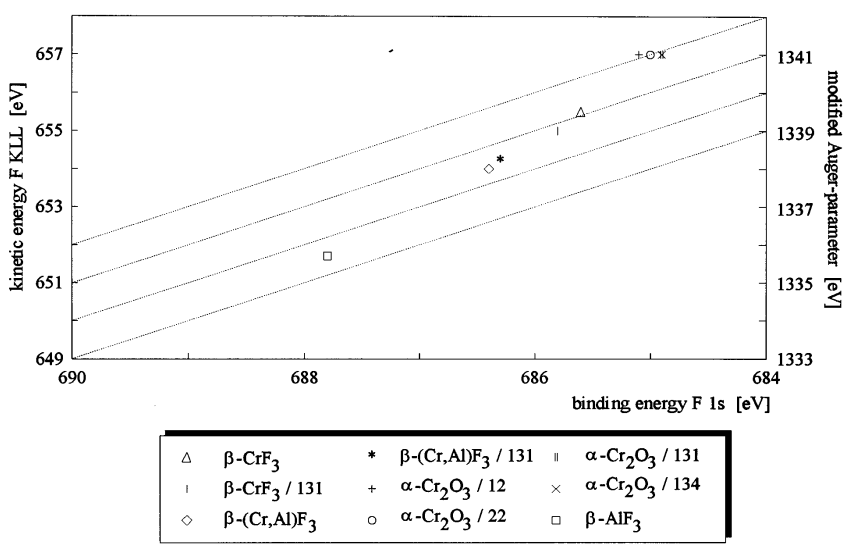

FIG. 8. Fluorine chemical state plot for Cr oxide and fluoride samples before and after activation with halocarbons (Static charge reference C 1*s*: 284.8 eV).

TABLE 3

Spectroscopic Data for Chromium Compounds from Literature

Author	Sample	Binding energy Cr $2p_{3/2}$	Reference
Shuttleworth (22)	Cr_2O_3	576.9 eV	C 1*s*: 285.0 eV
	$Cr(OH)_3$	577.6 eV	
	CrF_3	579.3 eV	
Carver *et al.* (23)	Cr_2O_3	577.0 eV	C 1*s*: 285.0 eV
	CrF_3	580.5 eV	
Merryfield *et al.* (24)	Cr_2O_3	576.2 eV	Au $4f_{7/2}$: 84.0 eV
	CrF_3	579.4 eV	
Paparazzo (25)	Cr_2O_3	576.6 eV	C 1*s*: 285.0 eV
Petkov *et al.* (26)	Cr_2O_3	576.6 eV	C 1*s*: 285.0 eV

rather high CCl_2F_2 conversion rates for the dismutation reaction which was used as the probe reaction. A significant activation effect was not obtained. In agreement with these results our XPS investigations did not reveal any hint of catalytically relevant changes of the surface characteristics.

A slightly different situation occurs for the bi-phasic β-(Cr, Al)F_3 samples used as catalysts. Due to the higher hydrolyzability of Cr–F bonds, partially hydrolyzed species, most probably Cr–O(H) species, are formed during the synthesis procedure (Table 4). The quantity of these chromium oxygen/hydroxyl species, observed with the bi-phasic β-(Cr, Al)F_3 sample, is significantly diminished from 27% to roughly 15% due to the activation procedure. On the other hand, the spectroscopic data obtained for F and the majority Cr species are not significantly influenced by the treatment (Figs. 7 and 8).

In the case of treated β-CrF_3 the XPS and XAES data are also similar to the untreated state of the surface. The shift of the Cr $2p_{3/2}$ binding energy to higher values is considered to be the effect of a replacement of surface OH groups in the precursor by fluoride during the reaction with HCFC-131a, thus giving fully fluorinated surroundings to the Cr surface atoms. Consistently we found an increase in the F/Cr surface concentration ratio from 2.8 to 3.2 due to treatments. The latter value equals the one obtained with crystalline α-CrF_3. Moreover, a decrease in the intensity of the hydroxyl group oxygen signal for treated chromia was found together with a slight chlorination of the surface.

TABLE 4

Surface Atomic Ratios of Reference Samples and Conditioned Precursors

Sample	O_{Ox}[a]/Me	O_{OH}[b]/Me	F/Cr	Cl/Cr	F/Al	Al/Cr
α-Cr_2O_3	2.0	0.1				
α-Cr_2O_3 with CFC-12	1.7	$\ll$0.1	0.17	0.20		
α-Cr_2O_3 with HCFC-22	1.8	0.1	0.15	0.12		
α-Cr_2O_3 with HCFC-131a	1.7	0.1	0.43	0.01		
α-Cr_2O_3 with HFC-134	1.6	0.1	0.43			
α-CrF_3	0.0	0.4	3.3			
β-CrF_3	0.0	0.6	2.8			
β-CrF_3 with HCFC-131a	0.07	0.3	3.2	0.09		
β-(Cr, Al)F_3	0.4 Cr	0.2 (Cr)	4.3	0.12	5.4	0.8
β-(Cr, Al)F_3 with HCFC-131a	0.5 (Cr)	$\ll$0.01 (Cr)	3.9	0.12	4.9	0.8
β-AlF_3	0.25	$\ll$0.01			2.3	

[a] Oxidic oxygen (O^{2-}).

[b] Unresolved contributions of OH^- and H_2O, adsorbed, or crystal water.

DISCUSSION

Activation of the Solids

To develop catalytic activity α-Cr_2O_3 has to be activated in a halocarbon gas stream. As a result of this treatment changes in the chemical composition and structural constitution occur at the surface of the solid. The heterogeneous solid gas reaction causes degradation reactions of the gas phase components and a partial halogenation of the chromia surface is exhibited.

Quite different behavior can be observed with the fluorides which are characterized by so-called HTB structures (β-CrF_3 and β-(Cr, Al)F_3). These samples are immediately catalytically active without any activation requirement. Obviously, these phases provide the structural conditions for the highly active surface sites which are necessary for the heterogeneous chlorine/fluorine exchange. The XPS spectra do not show any significant differences between the precursors and the treated samples. In contrast to that the stable α modification of CrF_3 reveals no evidence for catalytic activity. From these results it can be concluded that the activation of α-Cr_2O_3 leads to the formation of surface compounds which are, regarding their structure and chemical composition, very similar to that of the catalytic active HTB phases. With the alumina system we found very similar results (11, 12).

It is striking that the activation of α-Cr_2O_3 results in very similar quantitative XPS data even if different halocarbons are used. However, there are differences in the Cl to F ratio whereas the *integral* halogen content of the surface (sum of Cl^- and F^- contents) is in all cases very similar and seems to be nearly independent of the haloalkane species used for activation (Table 4). Thus, CH_2Cl–CCl_2F (HCFC-131a) treatment provides a significantly higher F-surface content than CCl_2F_2. Obviously, these differences are caused by the different reactivity of the gas phase. In the case of CCl_2F_2 the halogenation of the solid surface is mainly caused by an extended halogen exchange (OH/X and/or O/X exchange)

between the solid and the halocarbon and/or the reaction of the solid with the degradation products of CCl_2F_2 (HF or HCl). In contrast to that, HCFC-131a nearly completely splits off HF forming trichloroethylene (30).

$$CH_2Cl–CCl_2F \rightarrow CHCl{=}{=}CCl_2 + HF \qquad [7]$$

In this case HF acts as a strong fluorinating agent in agreement with the observed fluoride content of the surface (Table 4).

Structural Differences between α-CrF_3 and β-CrF_3

Besides differences in the catalytic behavior of the two fluoride phases also photoacoustic and TPD measurements reveal high Lewis acidity in the case of β-CrF_3 whereas Lewis acidity in the case of α-CrF_3 was not detectable. This indicates again remarkable differences in the surface environment of the metal cations. The question is whether these contrasting catalytic and surface properties of α-CrF_3 and β-CrF_3 can be explained by structural differences in the two phases.

The following is an attempt to give an explanation for these differences on the basis of distinctive structural differences between the two phases.

The catalytic and surface characterization data prove that there are obviously free, reactive sites for heterogeneous halogen exchange in the case of β-CrF_3 and that they completely disappear in the case of α-CrF_3. Both modifications contain $CrF_{6/2}$ octahedra, but they differ in the nature of the linking. In α-CrF_3 the fluoride anions are close-packed and (Fig. 9a) the chromium cations are situated in the octahedral holes. In the β-CrF_3 phase the $CrF_{6/2}$ octahedra are arranged in such a way that hexagonal channels parallel to the z axis are formed (Fig. 10a). The diameter of the channels is too small to explain the catalytic behavior of this phase by the entering of haloalkane molecules as is the case with zeolites. In addition to this fact, the acidic Cr^{3+} cations would be in any case protected by the F^- ions, as shown for the α-CrF_3. Construction of hypothetical surfaces for both modifications suggests significant different arrangements of chromium and could explain the contrasting behavior.

α-CrF_3. It can be seen from Fig. 9a that the chromium atoms are arranged at nearly the same level in the structure. No matter where one cuts through the structure, in every case one obtains a surface which is roughly planar and, what is especially important, where the larger fluoride ions occupy the outermost surface (cf. Fig. 9b). The Cr^{3+} cations are situated underneath this F^- layer. Therefore these coordinately unsaturated Cr^{3+} ions are sterically protected by the anions in such a way that an attack by the halogen atoms of a haloalkane molecule is impossible.

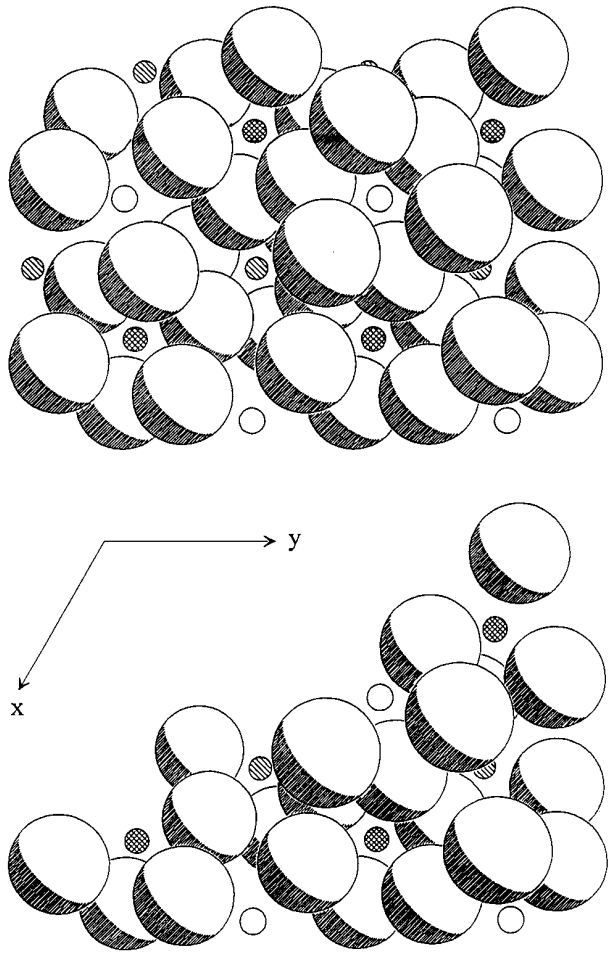

FIG. 9. Structure of α-CrF_3 (large circles, F atoms; ◯, Cr atoms at $z = 2/3$; ◯, Cr atoms at $z = 1/2$; Cr atoms at $z = 1/3$). (Upper part) projection in z direction; (lower part) cut through the structure in z direction.

β-CrF_3. The structural arrangements of Cr^{3+} and F^- ions are presented in Fig. 10a. A surface model from this structure obtained by minimizing the cleavage energy should pass through the hexagonal channels parallel to the z axis. However, doing this produces a hypothetical surface which is wave-shaped in the case of β-CrF_3 (Fig. 10b). The particularity of this surface is that the coordinatively unsaturated β-Cr^{3+} ions are situated now at the top of the waves. Due to this special arrangement the fluoride ions, in contrast to the alpha phase, are not able to protect the chromium sites sterically.

As a result, β-CrF_3, has reactive Lewis acidic sites and is able to be a catalytically active phase. This simple idea disregarded the possibility of relaxation processes at the surface, which clearly will occur. However, relaxation processes cannot change the whole character of the surface. We therefore conclude that the activity data correlate with the structurally defined surface metal atom environments.

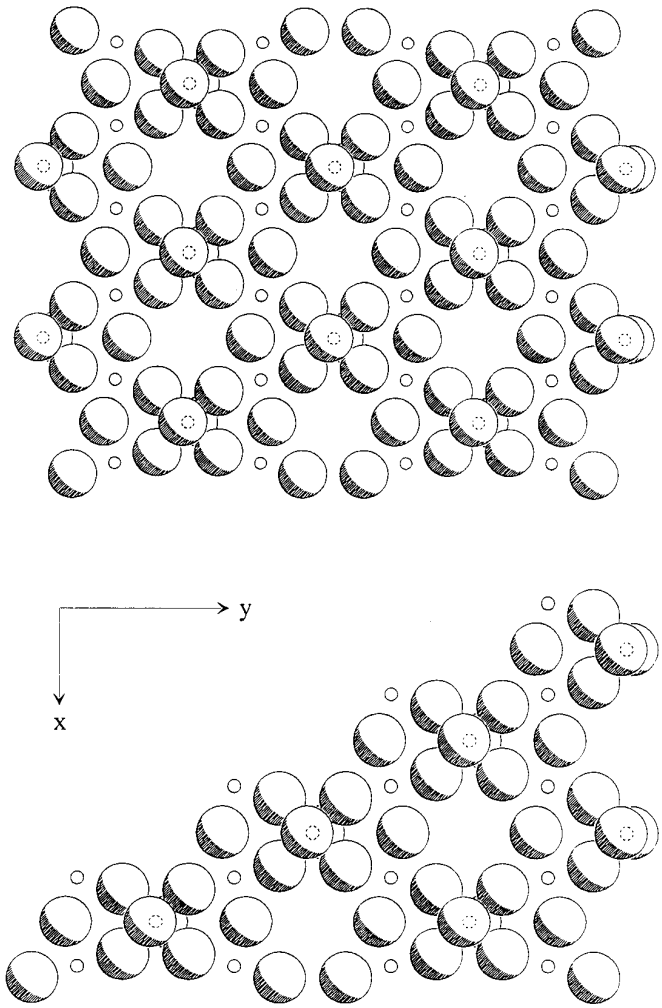

FIG. 10. Structure of β-CrF_3 (large circles, F atoms; small circles, Cr atoms). (Upper part) projection in z direction; (lower part) cut through the channels in z-direction.

ACKNOWLEDGMENTS

We gratefully acknowledge the financial support of the Deutsche Forschungsgemeinschaft and the Fonds der chemischen Industrie. We are grateful to Dr. S. Troyanov from the Moscow State University for discussion of fluoride structures.

REFERENCES

1. Manzer, L. E., PCT Int. Appl. WO 90 8755, 1990.
2. Wanzke, W., Siegemund, G., and Schmieder, W., European Patent Application EP 417 680, 1991.
3. Koyama, S., Homoto, Y., and Esaka, N., European Patent Application EP 446 869, 1991.
4. Cheminal, B., Lacroix, E., and Lantz, A., European Patent Application EP 486 333, 1992.
5. Brunet, S., Requieme, B., Matouba, E., Barrault, J., and Blanchard, M., *J. Catal.* **152**, 70 (1995).
6. Ballinger, T. H., and Yates, J. T., *J. Phys. Chem.* **96**, 1417 (1992).
7. Ballinger, T. H., Smith, R. S., Colson, S. D., and Yates, J. T., *Langmuir* **8**, 2473 (1992).
8. Thomson, J., Webb, G., and Winfield, J. M., *J. Chem. Soc. Chem. Commun.* 323 (1991).
9. Thomson, J., Webb, G., Winfield, J. M., Bonniface, D., Shortman, C., and Winterton, N., *Appl. Catal. Ser. A*, **97**, 67 (1993).
10. Hess, A., and Kemnitz, E., *J. Fluorine Chem.* in press.
11. Hess, A., Kemnitz, E., Lippitz, A., Unger, W. E. S., and Menz, D. H., *J. Catal.* **148**, 270 (1994).
12. Hess, A., and Kemnitz, E., *J. Catal.* **149**, 449 (1994).
13. Menz, D. H., and Bentrup, U., *Z. Anorg. Allg. Chem.* **613**, 108 (1992).
14. Menz, D. H., and Erhardt, B., *J. Thermal Anal.* **42**, 925 (1994).
15. Anthony, M. T., and Seah, M. P., *Surf. Interface Anal.* **6**, 94 (1984).
16. NIST Standard Reference Database 20 (NIST X-Ray Photoelectron Spectroscopy Database), Version 1.0, Data compiled and evaluated by C. D. Wagner. Natl. Inst. of Standards and Technology, Gaithersburg, 1989.
17. Grohmann, I., Kemnitz, E., Lippitz, A., and Unger, W. E. S., *Surf. Interface Anal.* **23**, 887 (1995).
18. Scofield, J. H., *J. Electron. Spectrosc. Realt. Phenom.* **8**, 129 (1976).
19. Kemnitz, E., Hass, D., and Grimm, B., *Z. Anorg. Allg. Chem.* **589**, 228 (1990).
20. De Pape, R., Le Bail, A., Lubin, F., and Ferey, G., *Rev. Chim. Miner.* **24**, 545 (1987).
21. Wagner, C. D., and Joshi, A., *J. Electron Spectrosc. Relat. Phenom.* **47**, 283 (1988).
22. Shuttleworth, D., *J. Phys. Chem.* **84**, 1629 (1980).
23. Carver, J. C., Schweitzer, G. K., and Carlson, T. A., *J. Phys. Chem.* **57**, 973 (1972).
24. Merryfield, R., McDaniel, M., and Parks, G., *J. Catal.* **77**, 348 (1982).
25. Paparazzo, E., *J. Electron Spectrosc. Relat. Phenom.* **43**, 97 (1987).
26. Petkov, K., Krustev, V., and Marinova, Ts., *Surf. Interface Anal.* **18**, 487 (1992).
27. Kohne, A., Thesis, Humboldt University, Berlin, 1994.
28. Hess, A., Thesis, Humboldt University, Berlin, 1994.
29. Kemnitz, E., and Niedersen, K.-U., *J. Catal.* **155**, 283 (1995).
30. Kohne, A., and Kemnitz, E., *J. Fluorine Chem.* **75**, 103 (1995).